

# Characterization of a Plasmoid in the Afterglow of a Supersonic Flowing Microwave Discharge

D. J. Drake<sup>1</sup>, S. Miller<sup>1</sup>, M. Nikolić<sup>1</sup>, S. Popović<sup>1</sup>, and L. Vušković<sup>1</sup>

<sup>1</sup>Department of Physics, Old Dominion University, 4600 Elkhorn Ave., Norfolk, VA 23529

We performed a detailed characterization a plasmoid in the afterglow region of an Ar supersonic microwave cavity discharge. The supersonic flow was generated using a convergent-divergent nozzle upstream of the discharge region. A cylindrical cavity was used to sustain a discharge in the pressure range of 100-600 Pa. Optical emission spectroscopy was used to observe populations of excited and ionic species in the plasmoid region.

## 1. Introduction

We describe in this report a plasmoid-like structure appearing as a secondary, downstream phenomenon coupled to the microwave cavity discharge in the supersonic flow in argon. The plasmoid is apparently sustained by a low-power surface wave which propagates along its surface and the surface of the containing quartz tube. Plasmoid formation is observed in pure argon in supersonic flow, while it is not sustained in the subsonic flow or in the mixture of argon with hydrogen (>1%). Some characteristics of the discharge suggest behavior similar to other surface microwave discharges [1], but the full interpretation requires inclusion of the aerodynamic arguments. For instance, the Abel-inverted line intensities of Argon ion lines have the characteristic contour profiles of the surface wave-sustained discharges. The fact that the plasmoid structure is detached from the plasmoid and depends on the flow velocity suggests the importance of aerodynamic mechanism.

## 2. Experimental Approach

The experimental set-up shown in Fig. 1 is a combination of supersonic flow tube and a microwave cavity discharge. Using an evacuated quartz tube at pressures of 1–3 Torr, supersonic flow was generated with a Mach 2 cylindrical convergent-divergent (de Laval) nozzle upstream of the cavity. We used a commercial microwave generator, operating in the S-band at 2.45 GHz, to sustain a cylindrical cavity discharge at power density between 0.5 and 4 W/cm<sup>3</sup>. Argon gas was fed into the stagnation chamber through a gas manifold. The gas flow was established by using a roots blower in conjunction with two roughing pumps. The capacity of the pumping system allowed a supersonic flow to be generated in a pressure range of 1 – 20 Torr.

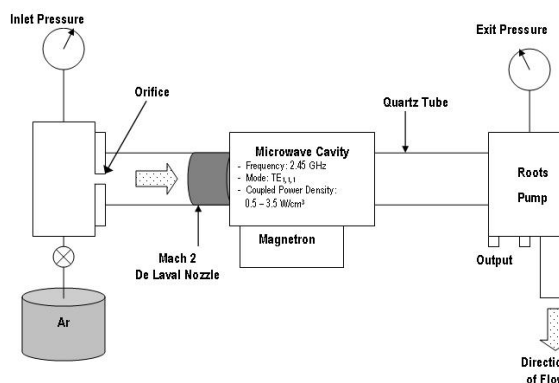


FIG. 1. Scheme of the supersonic flowing experiment.

We used optical emission spectroscopy as our primary diagnostic tool to observe the spectra of the excited states. Although there are uncertainties in this method, it is useful in these experiments since it is simple, nonintrusive, and *in situ*. In Fig. 2, we show that a CCD camera was used in conjunction with a spectrometer for measurement of the gas and electron temperature [2].

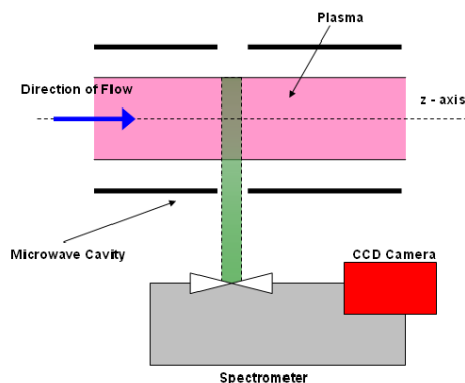


FIG. 2. Optical emission spectroscopy set-up.

The observed spectral frames were calibrated using a Spectra Physics Pen lamp and the intensity was calibrated using a Newport/Oriel absolute blackbody

irradiance source. Graphs of irradiance per count versus wavelength were calculated for the three spectrometer gratings. We determined the population of particular excited state transitions by using these graphs.

The populations of Ar excited states in a model free flow are shown in Fig. 3. By comparing the population values with a Boltzmann plot (straight line), we observe that at higher energies, the population decreased. This effect was more pronounced at the higher power density.

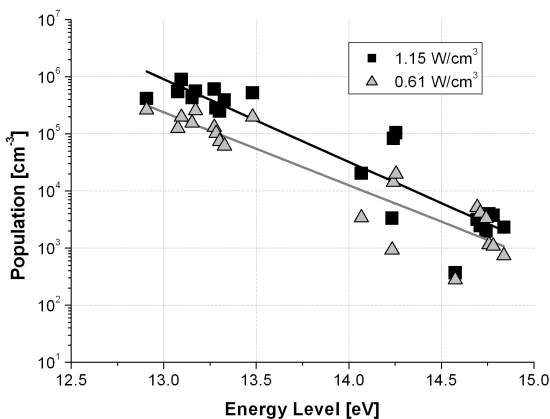


FIG. 3. Population of ArI states as a function of the energy level.

### 3. Analysis of a Plasmoid in the Afterglow Region

In the afterglow region, we observed the formation of a plasmoid, see Fig. 4.

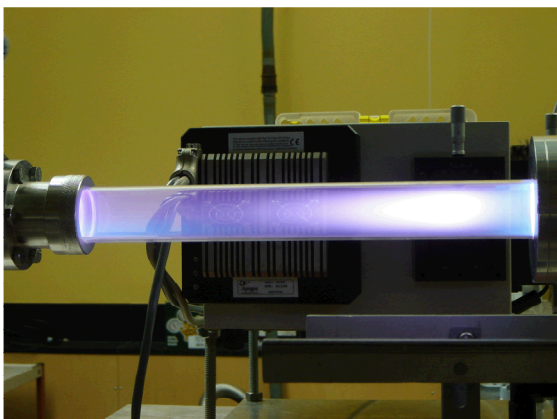


FIG. 4. Picture of the plasmoid in an Ar discharge at a pressure of 2.5 Torr and a power density of 1.45 W/cm<sup>3</sup>.

We made measurements of the populations of the Ar excited states in this region at 1.0 cm increments from the microwave cavity. In Fig. 5 we observe that the population of the Ar 4p[3/2] → 4s[3/2]<sup>o</sup> transition at 706.72 nm changes by an order of magnitude across the plasmoid region. In addition, to measurements along the axis of symmetry for the quartz tube, we measured the population at 0.3 cm increments vertically. The collected data was used to interpolate the change in the population over the entire plasmoid region and we present these results in Fig. 6. From the figure we see that the population of the excited states is greater at the head of the plasmoid. However there is also a distinctive separation of the ionic states in the plasmoid, one at a height of 0.7 cm and the other at 2.4 cm. This separation could be due to the fact that our plasmoid is more doughnut shaped.

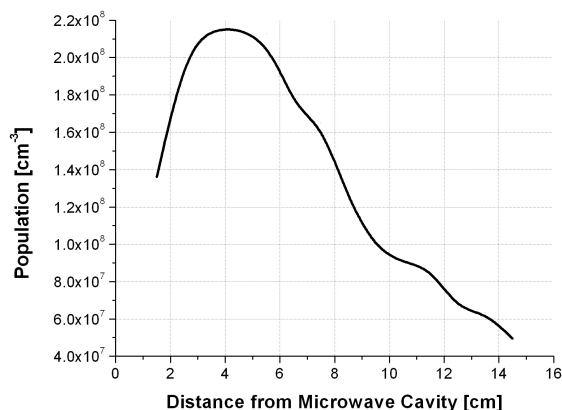


FIG. 5. Population of the ArI 4p[3/2] → 4s[3/2]<sup>o</sup> state at 706.72 nm along the axis of symmetry of the plasmoid as a function of the distance from the microwave cavity.

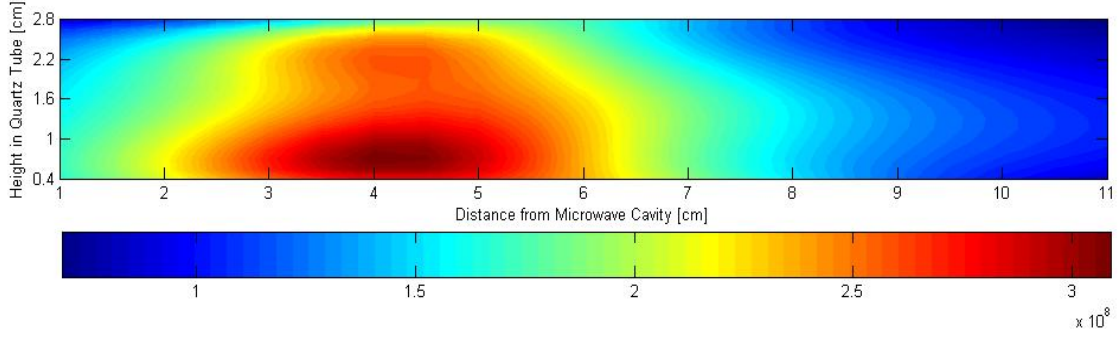


FIG. 6. Population of the ArI  $4p[3/2] \rightarrow 4s[3/2]^\circ$  state at 706.72 nm of the plasmoid as a function of the distance from the microwave cavity and the height in the quartz tube.

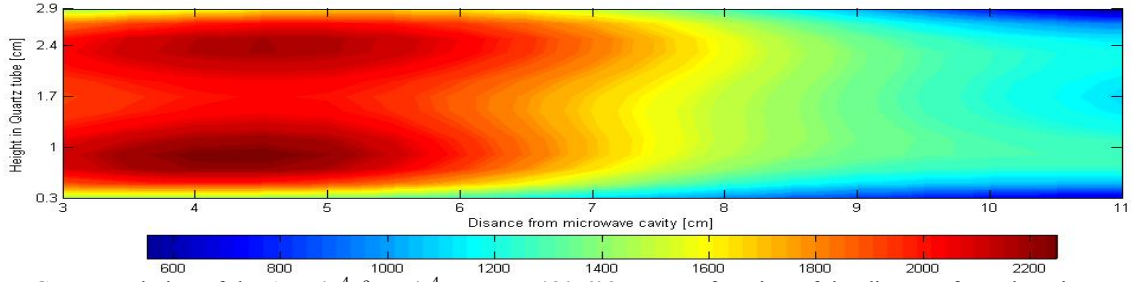


FIG. 7. Population of the ArII  $4p^4P^o \rightarrow 4s^4P$  state at 480.602 nm as a function of the distance from the microwave cavity.

We also measured the populations of the Ar II  $4p^4P^o \rightarrow 4s^4P$  state at 480.602 nm, see Fig. 7. As in the case of the lower energy transitions, we observe that population is greatest at the head of the plasmoid. In addition, we also observed two distinct peaks in the population like in the case of the Ar excited state.

The evaluated values of the population in Figs. 5-7 are based on the measured spectral line intensities,  $I(x)$ , in the discharge. However, measurements taken in the side-on direction were integrated over the entire depth of the discharge region. Assuming cylindrical symmetry, then the radial emission coefficient,  $\varepsilon(r)$ , is related to the measured intensities by the Abel transform,

$$I(x) = \int_{-y_0}^{y_0} \varepsilon(r) dy. \quad (1)$$

Inverting Eq. (1), provides a way to determine  $\varepsilon(r)$  from the experimental values of  $I(x)$ ,

$$\varepsilon(r) = -\frac{1}{\pi} \int_r^R \frac{I'(x)}{\sqrt{x^2 - r^2}} dx. \quad (2)$$

Here  $I'(x)$  is the first derivative of  $I(x)$  with respect to  $x$  and  $R$  is the plasma radius. Measurements of the spectral lines provide only discrete values of  $I(x)$ . Thus solutions of Eq. (2) can only be approximated. In addition, there is a discontinuity at  $x = r$  and  $\varepsilon(r)$  is dependent on  $I'(x)$ . To proceed, we assumed  $2N+1$  discrete points for the intensity distribution  $I(x_i)$ , where  $x_i = i \Delta x$  and  $i = -N \dots 0 \dots N$ . This distribution is used to find a  $N+1$  distribution  $\varepsilon(r_j)$ , where  $r_j = j \Delta r$  and  $j = 0 \dots N$ . In addition, we must assume that  $\Delta r = \Delta x$ ,  $r_0 = x_0 = 0$ , and  $r_N = x_N = R$ . Direct discretization [3] of Eq. (2) gives a good approximation of the values of  $\varepsilon(r_j)$  provided that  $I(x_i)$  has been previously interpolated and smoothed,

$$\varepsilon(r_j) = -\frac{1}{\pi} \sum_{i=j}^{N-1} \frac{I(x_{i+1}) - I(x_i)}{\sqrt{\left(x_i + \frac{\Delta x}{2}\right)^2 - r_j^2}}. \quad (3)$$

Applying Eq. (3) to the data in Fig. 7 we calculated the populations for the Ar II  $4p^4P^o \rightarrow 4s^4P$  state at 480.602 nm and present the results in Fig. 8. Once can see from the figure that the discharge seems to be located at the surface of the quartz tube.

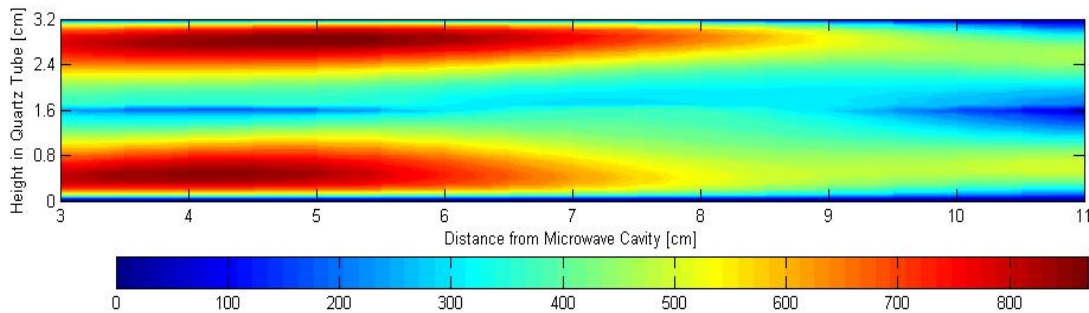


FIG. 8. Population of the ArII  $4p^4P^o \rightarrow 4s^4P$  state at 480.602 nm as a function of the distance from the microwave cavity.

In addition, we also observed the change in the plasmoid with pressure. In Fig. 9, we present the normalized population for the 706.72 nm line at 5.1, 2.4, and 1.5 Torr. From the figure we observe that the center of the plasmoid, where the population was largest, appeared to be moving closer to the cavity as the pressure is increased. This change in the location of the plasmoid was confirmed visually.

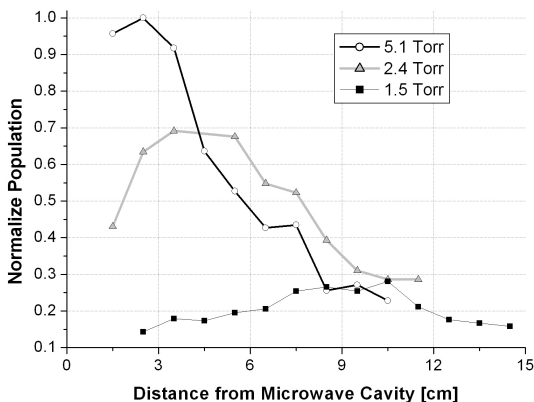


FIG. 9. Normalized population for the state at 706 nm at pressures of 5.1, 2.4, and 1.5 Torr.

The electron temperature distribution across the plasmoid region was obtained from the intensity ratio of an Ar atomic and an Ar ionic spectral line. For the discharge we used the Ar I  $5p[1/2] \rightarrow 4s^2[1/2]^o$  transition at 470.232 nm and the Ar II  $4p^2P^o \rightarrow 4s^2P$

state at 476.487 nm. Then by assuming chemical equilibrium between the Ar neutrals and Ar ions, we can apply the Saha-Boltzmann equation to determine the electron temperature ( $T_e$ ) [4],

$$\frac{N}{N^+} = \frac{N_e g}{2g^+} \left( \frac{h^2}{2\pi m_e k_B T_e} \right)^{3/2} \exp\left( \frac{E_{ion} - E_{exc}}{k_B T_e} \right). \quad (4)$$

Here  $N$  is the population of each state,  $g$  is the statistical weight,  $h$  is Planck's constant,  $m_e$  is the mass of the electron,  $k_B$  is the Boltzmann constant,  $E_{ion}$  is the ionization energy of the electron in the  $5p[1/2]$  state for the Ar I transition that is 1.2956 eV, and  $E_{exc}$  is the excitation energy of the  $4p^2P^o$  state of the Ar II transition that is 19.867 eV. We present these results in Fig. 10. From the figure we observe that the change in  $T_e$  was small over the entire plasmoid region ( $\Delta = \pm 90$  K), which would seem to indicate that this phenomenon is most likely due to aerodynamic effects.

To confirm these results we moved the microwave cavity at 1.0 cm increments. If the plasmoid is mostly due to aerodynamics, then the plasmoid would stay in the same place within the quartz tube. However, we found that the plasmoid moved with the microwave cavity, which indicated that there are electrodynamic effects causing this phenomenon as well as the aerodynamic effects.

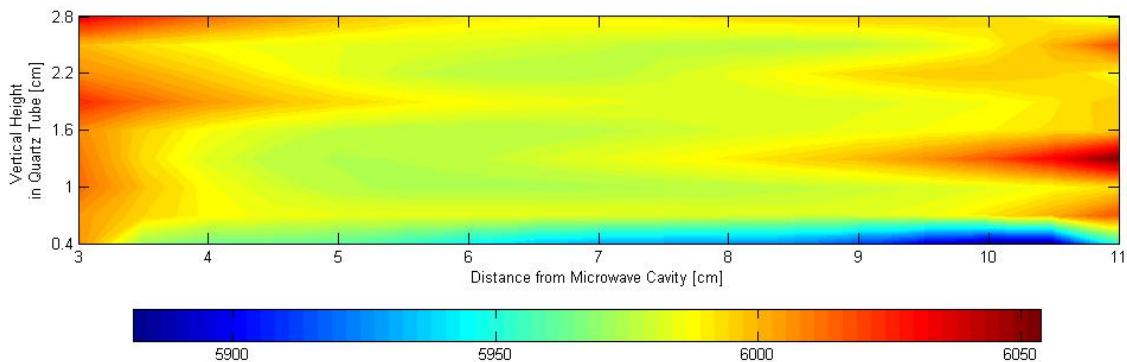


FIG. 10. Electron temperature as a function of the distance from the microwave cavity and the height in the quartz tube for an Ar discharge at a pressure of 2.5 Torr.

#### 4. Conclusions

Plasmoid formation in the supersonic flowing afterglow located downstream from the primary microwave cavity discharge was characterized by measuring the radial and axial distributions of Argon excited states and Argon ions. More experiments are being carried out on the plasmoid to understand the discharge parameters within the region, i.e. rotational temperature, vibrational temperature, electron density, and how the electrodynamic and aerodynamic effects combine to form this plasmoid.

#### 5. References

- [1] C. M. Ferreira and M. Moissan, *Physica Scripta*, **38**, 382 (1988).
- [2] D. J. Drake, S. Popović, and L. Vušković, *J. Appl. Phys.* **104**, 063305 (2008).
- [3] R. Álvarez, A. Rodero, and M. C. Quintero, *Spectrochim. Acta B* **57**, 1665 (2002).
- [4] A. Rodero, M. C. García, M. C. Quintero, A. Sola, and A. Gamero, *J. Phys. D: Appl. Phys.* **29**, 681 (1996).